metals

MDPI

Article

Microstructure and Compressive Behavior of Al–Y_2O_3 Nanocomposites Prepared by Microwave-Assisted Mechanical Alloying

Manohar Reddy Mattli [1], R. A. Shakoor [1,*], Penchal Reddy Matli [2] and Adel Mohamed Amer Mohamed [3]

[1] Center for Advanced Materials, Qatar University, Doha 2713, Qatar; manoharreddy892@gmail.com
[2] Department of Mechanical Engineering, National University of Singapore, Singapore 117576, Singapore; drlpenchal@nus.edu.sg
[3] Department of Metallurgical and Materials Engineering, Faculty of Petroleum and Mining Engineering, Suez University, Suez 43721, Egypt; adel.mohamed25@yahoo.com
* Correspondence: shakoor@qu.edu.qa; Tel.: +974-44036867

Received: 4 March 2019; Accepted: 3 April 2019; Published: 5 April 2019

Abstract: In this study, Al–Y_2O_3 nanocomposites were synthesized via mechanical alloying and microwave-assisted sintering. The effect of different levels of yttrium oxide on the microstructural and mechanical properties of the Al–Y_2O_3 nanocomposites were investigated. The density of the Al–Y_2O_3 nanocomposites increased with increasing Y_2O_3 volume fraction in the aluminum matrix, while the porosity decreased. Scanning electron microscopy analysis of the nanocomposites showed the homogeneous distribution of the Y_2O_3 nanoparticles in the aluminum matrix. X-ray diffraction analysis revealed the presence of yttria particles in the Al matrix. The mechanical properties of the Al–Y_2O_3 nanocomposites increased as the addition of yttria reached to 1.5 vol. % and thereafter decreased. The microhardness first increased from 38 Hv to 81 Hv, and then decreased to 74 ± 4 Hv for 1.5 vol. % yttria. The Al–1.5 vol. % Y_2O_3 nanocomposite exhibited the best ultimate compressive strength and yielded a strength of 359 ± 7 and 111 ± 5 MPa, respectively. The Al–Y_2O_3 nanocomposites showed higher hardness, yield strength, and compressive strength than the microwave-assisted mechanically alloyed pure Al.

Keywords: aluminum; yttrium oxide (yttria); mechanical alloying; microwave sintering; microstructure and mechanical properties

1. Introduction

Metal matrix composites (MMCs) find noteworthy applications in many engineering sectors due to their superior properties such as high strength, high-temperature capability, specific modulus, and good wear resistance compared to monolithic base materials. The mechanical performances of MMCs often show greater improvement than can be achieved by conventional strengthening methods in monolithic alloys [1–4].

Aluminum (Al)-based metal matrix composites (AMMCs) are an excellent choice for automotive, aerospace, defense, and nuclear power sectors because of their lightweight and favorable mechanical, thermal, and physical properties. Aluminum (Al)-based metal matrix composites are capable of achieving high strength, high-fatigue resistance, high-wear and corrosion resistance, and good compatibility with various manufacturing processes [5–8].

At present, ceramic particle-reinforced Al-matrix nanocomposites have been prepared primarily by mechanical alloying, forging, and casting routes [9–11]. Among these methods, mechanical alloying (MA) has been widely used to fabricate Al-matrix nanocomposites due its cost-effectiveness, simplicity,

and its ability to improve the properties vis-a-vis those of the unreinforced matrix [12,13]. There are many sintering techniques such as conventional, spark plasma, vacuum, and microwave sintering processes [14–17]. Among these techniques, the microwave sintering process is a heating method that offers the ability to balance the radiant and microwave heating effects. In this process, heat is generated within the sample by rapid oscillation of dipoles at microwave frequencies. Microwave sintering provides efficient internal heating, and energy is supplied directly to the material. Therefore, this process avoids the significant temperature gradient between the surface and interior. Microwave sintering is a high-technology heating process that can save both energy and time [18].

In AMMCs, the most common types of reinforcement that can be used are SiC, Si_3N_4, Y_2O_3, TiC, and Al_2O_3 [19–23]. Among these ceramics, Y_2O_3 was selected as the reinforcement to be used in this study due to its high strength, hardness, melting point, and thermal conductivity [24–26]. Yttria is an air-stable particle, white in color and solid in substance. By adding the yttria to the aluminum, the strength, corrosion resistance, and wear properties are improved [27]. Yttria is well sintered to a high density and low coefficient of thermal expansion, and has excellent strength properties [28,29]. According to the authors' knowledge, there are no reports in the literature on Al–Y_2O_3 nanocomposites processed by mechanical alloying and microwave sintering.

Therefore, in this current research, Al–Y_2O_3 nanocomposites were prepared by mechanical alloying and microwave heating, and the effect of Y_2O_3 addition on the microstructure and mechanical performance of Al–Y_2O_3 nanocomposites were investigated.

2. Materials and Methods

Pure Al (99.5% purity, with an average particle size of 10 μm) and Y_2O_3 nanoparticles (99.99% purity, with an average particle size of 50–70 nm) were purchased from Alfa Aesar (Tewksbury, MA, USA) and selected as raw materials for the synthesis of Al–Y_2O_3 nanocomposites.

Aluminum–yttria composites were prepared with 0, 0.5, 1.0, 1.5, and 2.0 vol. % yttria nanoparticle contents. The mixture of powders was blended at room temperature using a Planetary Ball Mill (PM 200) for 2 h, with a rotation speed of 200 rpm. No balls were used during the blending of powders. The mixed powder (~1.0 gm) was compacted into cylindrical pellets by applying a pressure of 50 MPa with a holding time of 1 min. The compacted cylindrical pellets were sintered in a microwave sintering furnace at a temperature of 550 °C with a heating rate of 10 °C/min and providing a dwell time of 30 min. The microwave furnace had an alumina insulation and silicon carbide susceptor. The silicon carbide susceptor was used to increase the heating rate and hybrid heating. Alumina insulation prevents heat loss and is used as well to protect the interior walls of the microwave oven. The compacted pellets were placed at the center of the cavity and sintering was conducted at the multimode cavity [30]. Figure 1 shows the schematic representation of the microwave sintering furnace.

The density of the sintered samples was calculated using Archimedes' principle. The porosity of the samples was calculated by the theoretical and experimental density of the composite samples. The X-ray diffraction (XRD, PANalytical X'pert Pro, PANalytical B.V., Almelo, The Netherlands) analysis was performed to identify the phases present in Al–Y_2O_3 nanocomposites. The XRD patterns were recorded in the 2θ range of 20–90° with a step size of 0.02° and a scanning rate of 1.5°/min. The microstructural characterization and determination of the distribution of the yttria nanoparticles in the aluminum matrix were carried out using scanning electron microscopy (SEM, JeolNeoscope JSM6000, Tokyo, Japan) and energy dispersive X-ray spectroscopy (EDS, Tokyo, Japan).

The microhardness of the Al–Y_2O_3 nanocomposites was determined using Vickers microhardness tester (MKV-h21, USA). Microhardness analysis was carried out to investigate the effect of yttria on the hardness of the Al–Y_2O_3 nanocomposite, carrying the load of 25 gf and a dwell time of 10 s, for each sample with an average of five successive indentations. Compressive strength analysis was performed at room temperature using a universal testing machine (Lloyd), under an engineering strain rate of 10^{-4}/s.

The respective data of each sample were obtained by an average of three successive values of test results. From the load–displacement curves, 0.2% offset compressive yield strength (CYS), ultimate compressive strength (UCS), and compressive strain were determined.

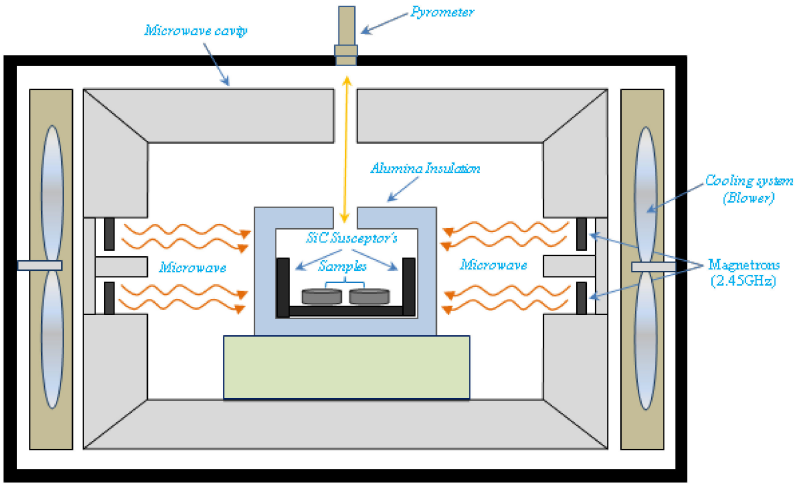

Figure 1. Schematic diagram of a microwave sintering furnace.

3. Results and Discussion

3.1. Density and Porosity of Al–Y_2O_3 Nanocomposites

Density and porosity values of the microwave sintered Al–Y_2O_3 nanocomposites with different contents of yttria in the Al matrix are shown in Table 1.

Table 1. Density and porosity of Al–Y_2O_3 nanocomposites.

Composition	Theoretical Density (g/cc)	Experimental Density (g/cc)	Porosity (%)
Pure Al	2.700	2.679 ± 0.005	0.78
Al–0.5 vol. % Y_2O_3	2.712	2.701 ± 0.004	0.41
Al–1.0 vol. % Y_2O_3	2.723	2.741 ± 0.007	0.33
Al–1.5 vol. % Y_2O_3	2.735	2.728 ± 0.006	0.26
Al–2.0 vol. % Y_2O_3	2.746	2.741 ± 0.008	0.18

It can be observed that the density of the composite gradually increased with the increase of the yttria content since the density of yttria (5.01 g\cc) is higher than that of Al (2.70 g\cc). Generally, the higher relative density of sintered samples influences the mechanical properties of the composites. The porosity of the composites decreased by increasing the amount of yttria content. The decrease in porosity with increasing yttria content shows that the presence of the hard yttria particles did not impair the densification of the Al powder [31]. Microwave heating was one of the main reasons for the low porosity of the synthesized composites.

3.2. XRD Analysis of Al–Y_2O_3 Nanocomposites

The X-ray diffraction (XRD) patterns of the microwave sintered pure Al and Al–Y_2O_3 nanocomposites with different amounts of Y_2O_3 are shown in Figure 2a. Figure 2b shows the enlarged patterns of the Al–1.5 vol. % Y_2O_3 nanocomposite. The XRD patterns clearly indicate the presence of Y_2O_3 nanoparticles in the Al composite matrix. Due to the small volume of yttria reinforcement present in these composites, the yttria peaks were very small compared to the aluminum matrix peaks. Also, it can be seen that the intensity of the yttria diffraction peaks increased with the increasing of yttria percentage. The XRD results show that the main elements of Al (higher peak) and Y_2O_3 (lower peak) are present in Al–Y_2O_3 nanocomposites.

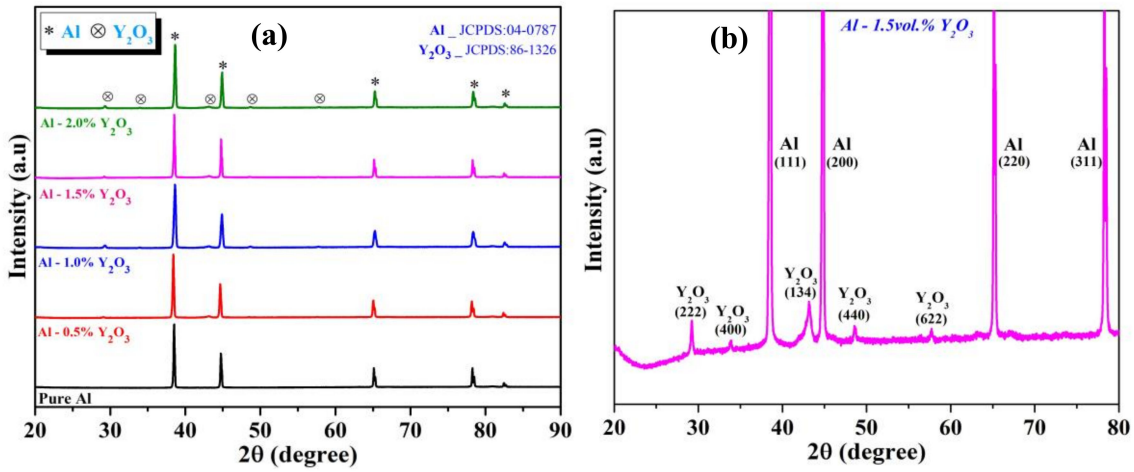

Figure 2. (**a**) X-ray diffraction (XRD) pattern of Al–Y_2O_3 nanocomposites, (**b**) enlarged pattern of Al–1.5vol. %Y_2O_3 nanocomposites [32,33].

3.3. SEM Analysis of Al–Y_2O_3 Nanocomposites

The SEM and EDS images of the microwave sintered Al–Y_2O_3 nanocomposites with different contents of yttria are shown in Figure 3. The results of microstructural characterization revealed that yttria particulates were present individually and in relatively smaller clusters indicating an improvement in their distribution. The EDS analysis confirms the aluminum and yttria particles present in the Al matrix. The EDS mapping spectrum of all nanocomposites were mainly composed of Al, Y, and O elements, as shown in Figure 3b,d,f. The microcracks were restricted by the presence of hard and homogeneous yttria particles in the Al-matrix and influenced the microstructure and mechanical properties of Al–Y_2O_3 nanocomposites. The specimen with 2 vol. % of yttria particles shows the decreasing of the interparticle distances as the concentration of the nanoparticles increased.

3.4. Microhardness of Al–Y_2O_3 Nanocomposites

Vickers microhardness was measured on all specimens to study the effect of Y_2O_3 content on the microhardness. Figure 4 shows the results of the microhardness of the Al–Y_2O_3 nanocomposites with different content of yttria. From the Table 2, the microhardness of the composite increased as the yttria increased of up to 1.5 vol. % and then decreased at 2.0 vol. % Y_2O_3. The considerable increase in hardness could be attributed to the presence of homogeneously distributed hard ceramic nanoparticles and dispersion hardening effect [34]. Al–2.0 vol. % Y_2O_3 nanocomposites show a decreased microhardness value, which was mainly due to the agglomeration of the yttria and increasing presence of clustering of yttria in the case of the Al matrix [35]. The microhardness of the microwave sintered samples in this study was found to be higher than the vacuum sintering and arc-melting samples [36].

The increment of microhardness in the composite materials was due to the presence of hard ceramic particles.

Table 2. Microhardness, yield strength, and ultimate compressive strength of Al–Y_2O_3 nanocomposites.

Composition	Microhardness (Hv)	YS (MPa)	UCS (MPa)	Compression Strain (%)
Pure Al	38 ± 3	69 ± 2	318 ± 5	>60
Al–0.5 vol. % Y_2O_3	46 ± 4	71 ± 4	329 ± 6	>60
Al–1.0 vol. % Y_2O_3	63 ± 2	87 ± 3	337 ± 3	>60
Al–1.5 vol. % Y_2O_3	81 ± 3	126 ± 5	374 ± 6	>60
Al–2.0 vol. % Y_2O_3	74 ± 5	111 ± 5	359 ± 7	>60

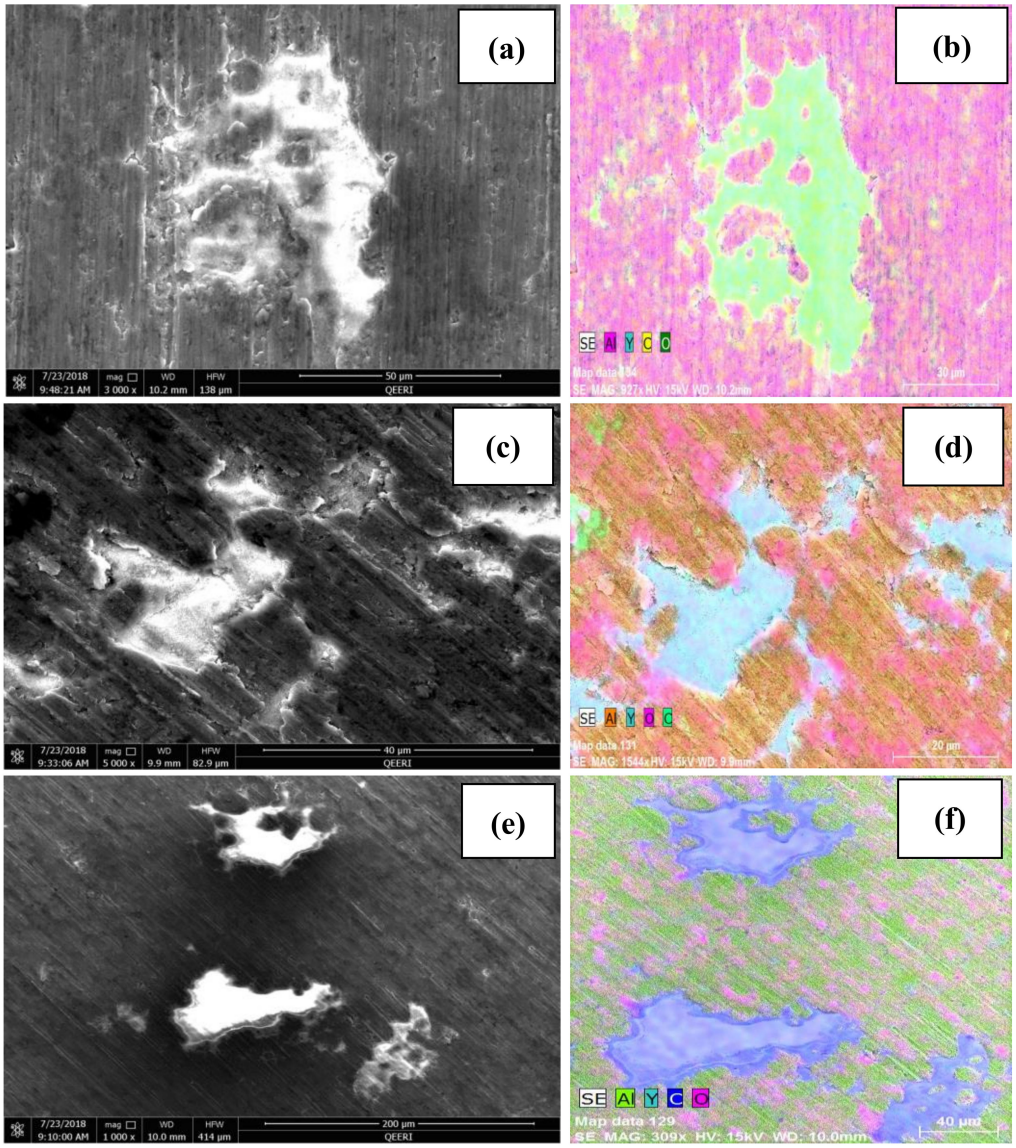

Figure 3. Typical micrographs and corresponding energy dispersion elemental mapping analysis of (**a**–**f**) Al–Y_2O_3 (1, 1.5, and 2 vol. %) nanocomposites.

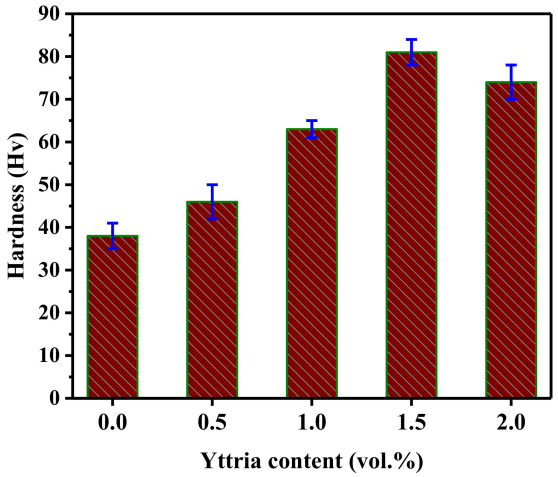

Figure 4. Microhardness of Al–Y_2O_3 nanocomposites.

3.5. Compressive Analysis of Al–Y_2O_3 Nanocomposites

The compressive test was conducted on the microwave sintered pure Al and Al–Y_2O_3 nanocomposites and strengths were compared. Figure 5a shows the engineering stress–strain curves of the Al–Y_2O_3 nanocomposites with different content of yttria. Figure 5b shows the corresponding mechanical data of Al–Y_2O_3 nanocomposites.

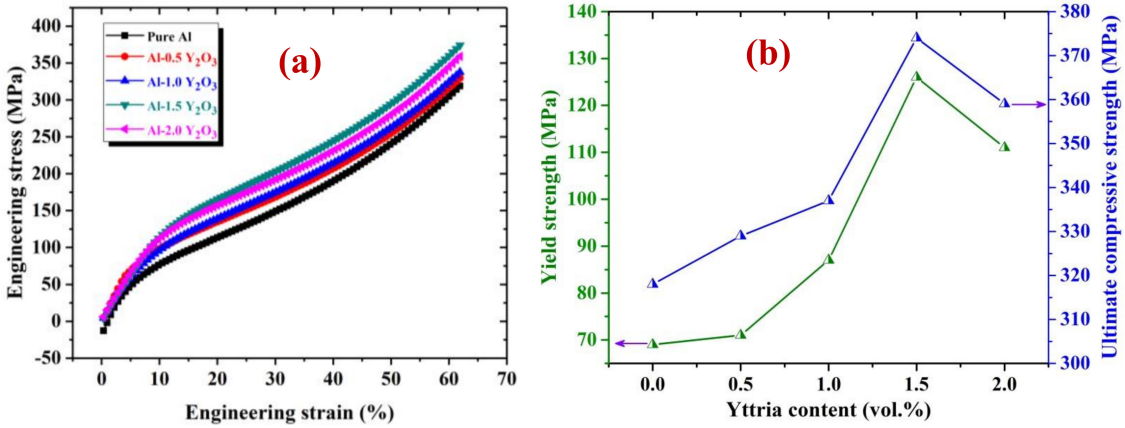

Figure 5. (**a**) The compressive stress–strain curves and (**b**) strength (yield and ultimate) of the Al–Y_2O_3 nanocomposites.

The yield strength and ultimate compressive strength of Al–Y_2O_3 nanocomposites show increased values up to 1.5 vol. % of yttria then decreased as shown in Table 2. Al–1.5 vol. %Y_2O_3 nanocomposites show the maximum yield strength (YS) of 126 ± 5 MPa and ultimate compressive strength (UCS) of 374 ± 6 MPa at a uniform strain of ~60%. These results show the improvement of mechanical properties of Al–Y_2O_3 nanocomposites compared to the pure Al. The increased mechanical properties of the Al–Y_2O_3 nanocomposites are attributed to the dispersion hardening effect and homogeneous distribution of hard reinforcements in the Al-matrix [37]. Al–2.0 vol. % Y_2O_3 nanocomposites show a decreased microhardness value, mainly due to the agglomeration of nanoparticles and grain growth [38]. Reinforcement amounts, density, heating mechanisms factors also govern the variation of the mechanical properties. However, compression properties of the microwave sintered Al–1.5 vol. % Y_2O_3 nanocomposites are interestingly superior to those of other reinforced AMMCs [39–43].

There are several strengthening mechanisms to enhance materials' mechanical properties like hardness and compressive strength of the composite materials. The strengthening of the composites is not only dependent on unique strengthening mechanisms, but it also depends on several strengthening mechanisms.

In the present study, the strengthening mechanism of the Al–Y_2O_3 nanocomposites mainly depended on dispersion hardening due to the hard yttria particles present in the aluminum matrix. The increase in strength and hardness may be attributable to Orowan strengthening [44,45].

3.6. Fractography of Al–Y_2O_3 Nanocomposites

Figure 6 shows the fracture surface images of microwave sintered pure Al and Al–Y_2O_3 nanocomposites under compressive loading. The SEM observations in nanocomposites show typical shear mode fractures and cracks obtained at a 45° to the fracture surfaces with respect to the compressive loading axis. It can be observed that the compressive deformations obtained in pure aluminum and aluminum composites with yttria are different, due to the work hardening behavior. The plastic deformations are restricted by the presence of the second phase in Al–Y_2O_3 nanocomposites [46].

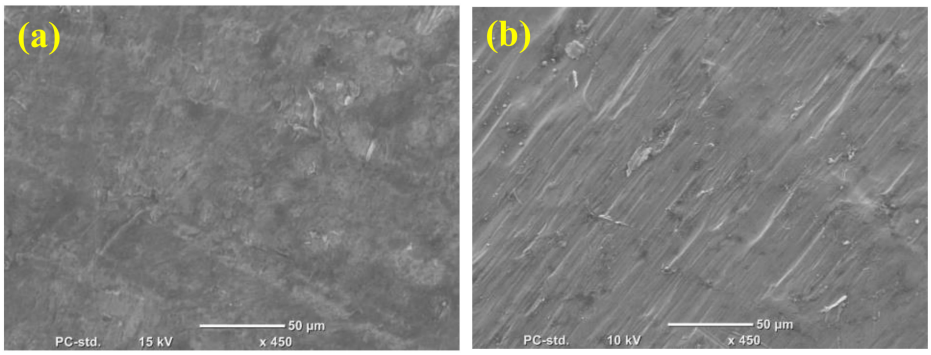

Figure 6. Compression fracture surfaces of (**a**) pure Al and (**b**) Al–1.5 vol. % Y_2O_3 nanocomposites.

4. Conclusions

The Al–Y_2O_3 nanocomposites were successfully synthesized by mechanical alloying and microwave sintering method. The influence of yttria nanoparticles on the microstructure and mechanical properties of the Al–Y_2O_3 nanocomposites were investigated in detail. The density of the composites increased with the increasing of yttria content while porosity decreased. The SEM analysis showed the homogeneous distribution of yttria particles in aluminum composites. The Al–Y_2O_3 nanocomposites exhibited better mechanical properties compared to pure Al. The optimum hardness (81 ± 3 Hv), yield strength (126 ± 5 MPa), and ultimate compression strength (374 ± 6 MPa) and compressive strain (~60%) values were obtained for the Al–1.5 vol. % Y_2O_3 nanocomposite. This significant enhancement in mechanical properties in Al–1.5 vol. % Y_2O_3 nanocomposites make them potential candidates for automotive applications.

Author Contributions: A.S. and A.M.A.M. proposed the original project and supervised the investigation. M.R.M. and P.R.M. performed the experiments, analyzed the data, and wrote the paper with assistance from all authors. All authors contributed to the discussions in the manuscript.

Funding: This publication was made possible by NPRP Grant 7-159-2-076 from the Qatar National Research Fund (a member of the Qatar Foundation). The Qatar National Library funded the publication cost of this article.

Conflicts of Interest: The authors declare no conflict of interest.

References

1. Warren, H.H. Metal matrix composites. In *Comprehensive Composite Materials*; Anthony, K., Carl, Z., Eds.; Pergamon Press: Oxford, UK, 2000; Volume 6, pp. 57–66.
2. Miracle, D.B. Metal matrix composites-from science to technological significance. *Compos. Sci. Technol.* **2005**, *65*, 2526–2540. [CrossRef]
3. Guild, F.J.; Taylor, A.C.; Downes, J. Composite materials. In *Encyclopedia of Maritime and Offshore Engineering*, 1st ed.; John Wiley & Sons, Inc.: Hoboken, NJ, USA, 2017.
4. Zweben, C. Composite materials. In *Mechanical Engineers' Handbook*; Kutz, M., Ed.; Wiley: Hoboken, NJ, USA, 2015.
5. Ghasali, E.; Hossen, A.; Agheli, M. WC-Co particles reinforced aluminum matrix by conventional and microwave sintering. *Mater. Res.* **2015**, *18*, 1197–1202. [CrossRef]
6. Sheasby, P.G.; Pinner, R. *The Surface Treatment and Finishing of Aluminum and Its Alloys*, 6th ed.; Finishing Publications Ltd.: Stevenage, UK; ASM International: Novelty, OH, USA, 2001; pp. 1–596.
7. Pardeep, S.; Satpal, S.; Dinesh, K. A study on the microstructure of aluminum matrix composites. *J. Asian Ceram. Soc.* **2105**, *3*, 240–244.
8. Manoj, S.; Deepak, D.D.; Lakhvir, S.; Vikas, C. Development of aluminium based silicon carbide particulate metal matrix composite. *J. Miner. Mater. Charact. Eng.* **2009**, *8*, 455–467.
9. Rana, R.S.; Purohit, R. Reviews on the influences of alloying elements on the microstructure and mechanical properties of aluminum alloys and aluminum alloy composites. *J. Sci. Eng. Res.* **2012**, *2*, 1–7.

10. Bharath, V.; Madev, N.; Auradi, V.; Kori, S.A. Preparation of 6061Al-Al_2O_3 MMC's by stir casting and evaluation of mechanical and wear properties. *Procedia Mater. Sci.* **2014**, *6*, 1658–1667. [CrossRef]
11. Narayan, S.; Rajeshkannan, A. Hardness, tensile and impact behavior of hot forged aluminum metal matrix composites. *J. Mater. Res. Technol.* **2017**, *6*, 213–219. [CrossRef]
12. Ghasali, E.; Pakseresht, A.; Ebadzadeh, T. Investigation on microstructure and mechanical behavior of Al–ZrB_2 composite prepared by microwave and spark plasma sintering. *Mater. Sci. Eng. A* **2015**, *627*, 27–31. [CrossRef]
13. Kong, J.; Xu, C.; Li, J.; Hou, H. Evolution of fractal features of pores in the compacting and sintering process. *Adv. Powder Technol.* **2011**, *22*, 439–442. [CrossRef]
14. Breval, E.; Cheng, J.P.; Agrawal, D.K.; Gigl, P.; Dennis, M.; Roy, R.; Papworth, A.J. Comparison between microwave and conventional sintering of WC/Co composites. *Mater. Sci. Eng. A* **2005**, *391*, 285–295. [CrossRef]
15. Shen, Z.; Johnsson, M.; Zhao, Z.; Nygren, M. Spark plasma sintering of alumina. *J. Mater. Process. Technol.* **2002**, *85*, 1921–1927. [CrossRef]
16. Jin, L.; Zhou, G.; Shimai, S.; Zhang, J.; Wang, S. ZrO_2-doped Y_2O_3 transparent ceramics via slip casting and vacuum sintering. *J. Eur. Ceram. Soc.* **2010**, *30*, 2139–2143. [CrossRef]
17. Rajkumar, K.; Aravindan, S. Microwave sintering of copper–graphite composites. *J. Mater. Process. Technol.* **2009**, *209*, 5601–5605. [CrossRef]
18. Reddy, M.P.; Ubaid, F.; Shakoor, R.A.; Gururaj, P.; Vyasaraj, M.; Mohamed, A.M.A.; Gupta, M. Effect of reinforcement concentration on the properties of hot extruded Al-Al_2O_3 composites synthesized through microwave sintering process. *Mater. Sci. Eng. A* **2017**, *696*, 60–69. [CrossRef]
19. Reddy, M.P.; Ubaid, F.; Shakoor, R.A.; Gururaj, P.; Vyasaraj, M.; Mohamed, A.M.A.; Gupta, M. Enhanced performance of nano-sized SiC reinforced Al metal matrix nanocomposites synthesized through microwave sintering and hot extrusion techniques. *Prog. Nat. Sci. Mater.* **2017**, *27*, 607–614. [CrossRef]
20. Wang, M.; Wang, D.; Kups, T.; Schaaf, P. Size effect on mechanical behavior of Al/Si_3N_4 multilayers by nanoindentation. *Mater. Sci. Eng. A* **2015**, *644*, 275–283. [CrossRef]
21. Kim, C.S.; Kim, I.H. Effect of Al and Y_2O_3 on mechanical properties in mechanically alloyed nanograin Ni-based alloys. *J. Nanosci. Nanotechnol.* **2105**, *15*, 6160–6163. [CrossRef]
22. Karantzalis, A.E.; Wyatt, S.; Kennedy, A.R. The mechanical properties of Al-TiC metal matrix composites fabricated by a flux-casting technique. *Mater. Sci. Eng. A* **1997**, *237*, 200–206. [CrossRef]
23. Hossein-Zadeh, M.; Razavi, M.; Mirzaee, O.; Ghaderi, R. Characterization of properties of Al–Al_2O_3 nano-composite synthesized via milling and subsequent casting. *J. King Saud Univ. Eng. Sci.* **2013**, *25*, 75–80. [CrossRef]
24. Ianos, R.; Babuta, R.; Lazau, R. Characteristics of Y_2O_3 powders prepared by solution combustion synthesis in the light of a new thermodynamic approach. *Ceram. Int.* **2014**, *40*, 12207–12211. [CrossRef]
25. Chaim, R.; Shlayer, A.; Estournes, C. Densification of nanocrystalline Y_2O_3 ceramic powder by spark plasma sintering. *J. Eur. Ceram. Soc.* **2009**, *29*, 91–98. [CrossRef]
26. Kakuoz, Y.B.; Serivalsatit, K.; Kokuoz, B.; Geiculescu, O.; McCormick, E.; Ballato, J. Er-doped Y_2O_3 nanoparticles: A comparison of different synthesis methods. *J. Am. Ceram. Soc.* **2009**, *92*, 2247–2253. [CrossRef]
27. Bouaeshi, W.B.; Li, D. Effects of Y_2O_3 addition on microstructure, mechanical properties, electrochemical behavior, and resistance to corrosive wear of aluminum. *Tribol. Int.* **2007**, *40*, 188–199. [CrossRef]
28. Cho, J.; Harmer, M.P.; Chan, H.M.; Rickman, J.M.; Thompson, A.M. Effect of yttrium and lanthanum on the tensile creep behavior of aluminum oxide. *J. Am. Ceram. Soc.* **1993**, *28*, 6466–6473. [CrossRef]
29. Borovkova, L.B.; Lukin, E.S.; Poluboyarinov, D.N.; Sapozhnikova, E.B. Sintering and properties of yttrium oxide ceramics. *Refract. Ind. Ceram.* **1970**, *11*, 717–722. [CrossRef]
30. Ranjan, S. Sintering and Mechanical Properties of Alumina-Yttrium Aluminate Composites. Ph.D. Thesis, National Institute of Technology, Rourkela, India, May 2015.
31. Meena, K.L.; Manna, A.; Banwait, S.S.; Jaswanti, D. An analysis of mechanical properties of the developed Al/SiC-MMC's. *Am. J. Mech. Eng.* **2013**, *1*, 14–19. [CrossRef]
32. Vamsi Krishna, M.; Xavior, M.A. Experiment and statistical analysis of end milling parameters for al/sic using response surface methodology. *Int. J. Eng. Technol.* **2015**, *7*, 2274–2285.

33. Dong, G.; Chi, Y.; Xiao, X.; Liu, X.; Qian, B.; Ma, Z.; Wu, E.; Zeng, H.; Chen, D.; Qiu, J. Fabrication and optical properties of Y_2O_3: Eu^{3+} nanofibers prepared by electrospinning. *Opt. Express* **2009**, *17*, 22514–22519. [CrossRef]
34. Reddy, M.P.; Himyan, M.A.; Ubaid, F.; Shakoor, R.A.; Gururaj, P.; Vyasaraj, M.; Mohamed, A.M.A.; Gupta, M. Enhancing thermal and mechanical response of aluminium using nanolength scale TiC reinforcement. *Ceram. Int.* **2018**, *44*, 9247–9254. [CrossRef]
35. Hassan, S.F.; Gupta, M. Development of nano-Y_2O_3 containing magnesium nanocomposites using solidification processing. *J. Alloy Compd.* **2007**, *429*, 176–183. [CrossRef]
36. Zhao, N.Q.; Jiang, B.; Du, X.W.; Li, J.J.; Shi, C.S.; Zhao, W.X. Effect of Y_2O_3 on the mechanical properties of open cell aluminum foams. *Mater. Lett.* **2006**, *60*, 1665–1668. [CrossRef]
37. Reddy, M.P.; Ubaid, F.; Shakoor, R.A.; Parande, G.; Vyasaraj, M.; Yusuf, M.; Mohamed, A.M.A.; Gupta, M. A comparative study of structural and mechanical properties of Al-Cu composites prepared by vacuum and microwave sintering techniques. *J. Mater. Res. Technol.* **2017**, *7*, 165–172.
38. Pasquale, C.; Farhad, J.; Ali, S.; Behzad, S. Influence of SiO_2 nanoparticles on the microstructure and mechanical properties of Al matrix nanocomposites fabricated by spark plasma sintering. *Compos. Part B Eng.* **2108**, *146*, 60–68.
39. Mahmut, C.S.; Gürbüz, M.; Koç, E. Fabrication and characterization of SiC and Si_3N_4 reinforced aluminum matrix composites. *Univers. J. Mater. Sci.* **2017**, *5*, 95–101.
40. Pakdel, A.; Farhangi, H.E. Effect of extrusion process on ductility and fracture behavior of SiCp/aluminum alloy composites. Proceedings of 8th International Fracture Conference, Istanbul Turkey, 7–9 November 2007.
41. Moustafa, M.M.M.; Omayma, A.E.; Abdelhameed, W.A. Effect of alumina particles addition on physico-mechanical properties of Al-matrix composites. *Open J. Metal* **2013**, *3*, 72–79.
42. Ehsan, G.; Masoud, A.; Touradj, E.; Amir, H.P.; Ali, R. Investigation on microstructural and mechanical properties of B4C–aluminum matrix composites prepared by microwave sintering. *J. Mater. Res. Technol.* **2015**, *4*, 411–415.
43. Hasan, K.I.; Aboozar, T.; Ali, M.; Abbas, G. Development of an aluminum/amorphous nano-SiO_2 composite using powder metallurgy and hot extrusion processes. *Ceram. Int.* **2017**, *43*, 14582–14592.
44. Zeng, X.; Liu, W.; Xu, B.; Shu, G.; Li, Q. Microstructure and mechanical properties of Al-SiC nanocomposites synthesized by surface-modified aluminium powder. *Metals* **2018**, *8*, 253. [CrossRef]
45. Ramezanalizadeh, H.; Emamy, M.; Shokouhimehr, M. A novel aluminum based nanocomposite with high strength and good ductility. *J. Alloys Compd.* **2015**, *649*, 461–473. [CrossRef]
46. Reddy, M.P.; Ubaid, F.; Shakoor, R.A.; Parande, G.; Vyasaraj, M.; Yusuf, M.; Mohamed, A.M.A.; Gupta, M. Improved properties of Al–Si_3N_4 nanocomposites fabricated through a microwave sintering and hot extrusion process. *RSC Adv.* **2017**, *7*, 34401–34410.